Scientific Report

SOURCE DATA | TRANSPARENT PROCESS | OPEN ACCESS

EMBO reports

Mad1 contribution to spindle assembly checkpoint signalling goes beyond presenting Mad2 at kinetochores

Stephanie Heinrich, Katharina Sewart[†], Hanna Windecker[‡], Maria Langegger, Nadine Schmidt, Nicole Hustedt[§] & Silke Hauf[*,†]

Abstract

The spindle assembly checkpoint inhibits anaphase until all chromosomes have become attached to the mitotic spindle. A complex between the checkpoint proteins Mad1 and Mad2 provides a platform for Mad2:Mad2 dimerization at unattached kinetochores, which enables Mad2 to delay anaphase. Here, we show that mutations in Bub1 and within the Mad1 C-terminal domain impair the kinetochore localization of Mad1:Mad2 and abrogate checkpoint activity. Artificial kinetochore recruitment of Mad1 in these mutants co-recruits Mad2; however, the checkpoint remains non-functional. We identify specific mutations within the C-terminal head of Mad1 that impair checkpoint activity without affecting the kinetochore localization of Bub1, Mad1 or Mad2. Hence, Mad1 potentially in conjunction with Bub1 has a crucial role in checkpoint signalling in addition to presenting Mad2.

Keywords fission yeast; kinetochore; Mad1; mitosis; spindle assembly checkpoint

Subject Categories Cell Cycle; Chromatin, Epigenetics, Genomics & Functional Genomics

DOI 10.1002/embr.201338114 | Received 16 October 2013 | Revised 8 January 2014 | Accepted 9 January 2014 | Published online 28 January 2014

EMBO Reports (2014) 15, 291–298

See also: **T Kruse *et al*** (March 2014)

Introduction

Mad1 is part of the spindle assembly checkpoint, a conserved mitotic signalling pathway that protects genome integrity by monitoring chromosome attachment to the mitotic spindle and delaying anaphase until all chromosomes have achieved proper attachment [1]. Mad1 forms a tetrameric complex with the checkpoint protein Mad2 [2]. At unattached kinetochores, Mad1-bound Mad2 dimerizes with soluble Mad2 to induce binding of the latter to Cdc20 [1,3], an essential co-activator of the anaphase-promoting complex/cyclosome (APC/C) [4]. This enables binding of Mad3 (BubR1 in many organisms) to Cdc20 to form the mitotic checkpoint complex (MCC), which is a potent inhibitor of the APC/C [4–6]. In *S. pombe*, the kinases Ark1 and Mph1, as well as Bub1 and Bub3, are required to bring Mad1:Mad2 to unattached kinetochores [7]. Similar dependencies exist in other organisms [1]. Consistent with the important role of the Mad1:Mad2 complex in initiating Cdc20 inhibition, preventing the Mad1:Mad2 interaction abolishes checkpoint activity [8–11]. Hence, Mad1 is important to present Mad2 at unattached kinetochores.

Mad1 has approximately 80 kDa; yet, the stretch that binds Mad2 is <20 amino acids long. This raises the question whether the remaining parts only have a structural role. The Mad1 part N-terminal to the Mad2-binding site is predicted to form a long coiled-coil. The structure of the C-terminal end of this coiled-coil (α1) together with the Mad2-binding site bound to Mad2 as well as a C-terminal helix (α2) indicated that α1 mediates Mad1 dimerization [2]. Another structure of the C-terminal part following α2 showed another intermolecular coiled-coil (α3) and a globular head [12] (see Figs 1A and 4A). The Mad1 C-terminus has repeatedly been implicated in kinetochore binding [12–14]; some studies have suggested a role for the N-terminus [15,16]. Budding yeast Mad1 interacts with Bub1, which requires a conserved motif (RLK, Arg-Leu-Lys) in the Mad1 α3 helix [17] and a conserved stretch in Bub1 [18]. This interaction is important for checkpoint activity [17], and in human cells, the RLK motif is required for kinetochore localization of Mad1 [12]. Overall, these observations indicate that the structured parts of Mad1 are required to bring the Mad1:Mad2 complex to kinetochores to allow checkpoint signalling, potentially through an interaction between Mad1 and Bub1.

Here, we show using fission yeast that the Mad1 C-terminus promotes checkpoint activity in a way that is independent of its role in bringing the Mad1:Mad2 complex to kinetochores.

Friedrich Miescher Laboratory of the Max Planck Society, Tübingen, Germany
*Corresponding author. Tel: +1 540 231 7318; Fax: +1 540 231 2606; E-mail: silke.hauf@vt.edu
[†]Current address: Department of Biological Sciences and Virginia Bioinformatics Institute, Virginia Polytechnic Institute and State University, Blacksburg, VA, USA
[‡]Current address: Institute of Molecular Biology (IMB), Mainz, Germany
[§]Current address: Friedrich Miescher Institute, Basel, Switzerland

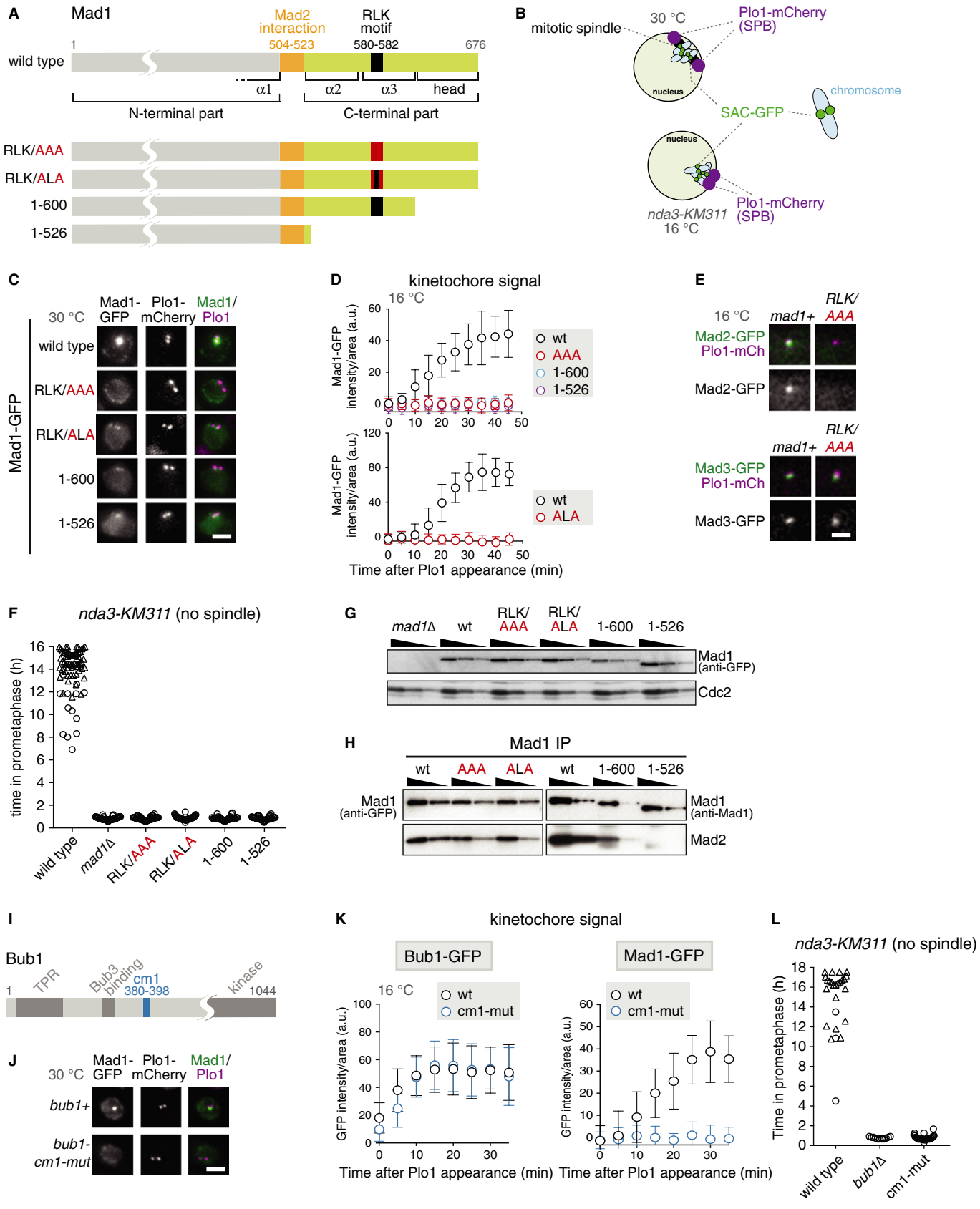

Figure 1. The Mad1 RLK motif and Bub1-cm1 are required for Mad1 kinetochore localization and checkpoint activity.

A Domain structure of Mad1; point mutations and truncations employed in this study.

B Schematic of fission yeast nuclei in prometaphase. Shown are the three chromosomes (light blue), the mitotic spindle (black) and kinetochores decorated with GFP-tagged SAC components (green). Plo1-mCherry (purple) is specifically recruited to spindle pole bodies (SPBs) in mitosis [37]. In interphase and early mitosis, kinetochores cluster at SPBs. In the conditional *nda3-KM311* tubulin mutant, microtubule formation is impaired at restrictive temperature (16°C) and spindle pole bodies are unable to separate. Signals from the three chromosomes can typically not be microscopically resolved at early mitosis.

C Cells expressing *plo1+-mCherry*, *nda3-KM311* and the indicated Mad1-GFP fusion proteins were grown at the permissive temperature for *nda3-KM311* (30°C). Representative nuclei of mitotic cells are shown; Plo1 was used as marker for mitosis (scale bar: 2 μm; see Supplementary Fig S1A for a larger field of view).

D The same strains as in (C) were analysed at the restrictive temperature for *nda3-KM311* (16°C), which prevents microtubule formation. Cells were followed by live-cell microscopy and the Mad1-GFP signals were quantified at the kinetochore as cells entered mitosis (a.u. = arbitrary units; error bars = s.d.; $n \geq 20$ cells).

E Cells expressing *plo1+-mCherry*, *nda3-KM311*, the indicated GFP fusion proteins and either wild-type Mad1 (*mad1+*) or *mad1-RLK/AAA* were imaged at 16°C. Representative nuclei of mitotic cells are shown. Scale bar: 2 μm.

F Cells expressing *plo1+-mCherry* and *nda3-KM311* and the indicated mutations or truncations in *mad1* were analysed by live-cell imaging at 16°C. The time that each cell spent in prometaphase was determined by the localized Plo1-mCherry signal at SPBs (circle). Cells that had not yet exited mitosis when filming stopped are indicated by triangles.

G Immunoblotting of cell extracts using anti-GFP (to detect the Mad1-GFP fusion proteins) and anti-Cdc2 (loading control) antibodies. A dilution series was loaded for each strain to compare intensities.

H Anti-Mad1 immunoprecipitations of the indicated strains were analysed for the presence of Mad1 and Mad2 using anti-GFP (left), anti-Mad1 (right) and anti-Mad2 antibodies. Input and flow through are shown in Supplementary Fig S1C.

I Domain structure of Bub1 (TPR: tetratricopeptide repeats; Bub3 binding: Bub3-binding motif, also called GLEBS; cm1: conserved motif 1; kinase: kinase domain).

J Cells expressing *mad1+-GFP*, *plo1+-mCherry*, *nda3-KM311* and either wild-type Bub1 (*bub1+*) or the Bub1-cm1-mutant (*bub1-cm1-mut*) were imaged at 30°C as in (C). Representative nuclei of mitotic cells are shown (scale bar: 2 μm; see Supplementary Fig S1H for a larger field of view). The Bub1-cm1 mutant contains aa changes S381A, T383A and T386A (alignment in Supplementary Fig S1E). The cellular abundance of wild-type and mutant Bub1-GFP was similar (Supplementary Fig S1F).

K Bub1-GFP or Mad1-GFP signals were quantified at the kinetochore as in (D) (a.u. = arbitrary units; error bars = s.d.; $n \geq 24$ cells for Bub1-GFP, $n \geq 18$ cells for Mad1-GFP).

L Checkpoint function of the indicated strains was analysed as in (F).

Source data are available online for this figure.

Results and Discussion

Mad1-RLK motif and Bub1-conserved motif 1 are required for kinetochore localization of Mad1 and checkpoint activity

To assess potential roles of Mad1 apart from Mad2-binding, we focused on the RLK motif (amino acid (aa) 580–582) within α3 [17]. When we mutated all motif residues to alanine in *S. pombe*, kinetochore localization of Mad1 and Mad2 was impaired (Fig 1A, C–E), whereas localization to the nuclear envelope stayed intact (Supplementary Fig S1A and D). Checkpoint activity was lost in the Mad1-RLK/AAA mutant (Fig 1F), although kinetochore localization of Ark1, Bub1, Bub3 and Mad3 was preserved (Fig 1E, Supplementary Fig S1B) and although Mad1-RLK/AAA was present at normal levels (Fig 1G) and the Mad1:Mad2 interaction was intact (Fig 1H). This suggests that the failure to bring Mad1:Mad2 to kinetochores causes the checkpoint defect. A similar loss of Mad1 localization and checkpoint activity occurred when only the outward-facing amino acids R and K of the RLK motif were mutated or when the C-terminus was truncated (Fig 1). The latter supports results from budding yeast [19]. Like RLK/AAA, the RLK/ALA mutation preserved Mad2 interaction, whereas truncation of the C-terminus led to a gradual loss of this interaction (Fig 1H). Although the Mad1 C-terminus was necessary for kinetochore binding (Fig 1C and D), it did not seem sufficient (Supplementary Fig S2). In contrast to the C-terminus, the Mad1 N-terminus was required for nuclear envelope localization, but was at least partly dispensable for kinetochore localization (Supplementary Fig S2).

The RLK motif has been implicated in binding to Bub1 in budding yeast [17,18], which involves a region of Bub1 that contains the "conserved motif 1" (cm1; [20]). Indeed, mutation of Bub1-cm1 phenocopied Mad1-RLK mutants (Fig 1I–L). Bub1 itself (Fig 1K) as well as Bub3 and Mad3 (Supplementary Fig S1I) still localized to kinetochores, but Mad1 and Mad2 were strongly reduced (Fig 1J and K, Supplementary Fig S1I) and cells lacked checkpoint activity (Fig 1L). We conclude that the C-terminus of Mad1 (with the RLK motif) and Bub1-cm1 are involved in recruiting Mad1 to kinetochores and both regions are important for checkpoint function.

The Mad1 RLK motif and Bub1-cm1 promote checkpoint activity independently of their role in Mad1 kinetochore localization

Since Bub1 and Mad1 have been observed to interact in budding yeast [17], it is conceivable that Bub1 and Mad1 interact through cm1 and RLK motif and that this interaction is required for Mad1 kinetochore localization and checkpoint activity. Surprisingly, we were unable to detect an interaction between these two proteins when immunoprecipitating either of them from cells with an active checkpoint (Supplementary Fig S3A and B), similar to the situation in human cells [12]. To test whether the loss of checkpoint activity in the Mad1-RLK/AAA or Bub1-cm1 mutant (Fig 1F and L) is at all related to the loss of Mad1 from kinetochores, we tested checkpoint activity after artificially recruiting Mad1 to kinetochores through fusion to the kinetochore protein Mis12 (Fig 2). Although the levels of tethered Mad1 at unattached kinetochores were slightly lower than for wild-type Mad1 (Fig 2E and F), the checkpoint was functional at least in a large fraction of the cells (Fig 2B and D). Tethering of Mad1-RLK/AAA, however, did not provide checkpoint activity (Fig 2B), even though Mad2 was co-recruited to the kinetochore at similar levels as in tethered wild-type Mad1 (Fig 2F). Similarly, artificially recruiting Mad1 in either *bub1Δ* or *bub1-cm1* cells did not restore the checkpoint (Fig 2D and E). This suggests that Bub1-cm1 and the Mad1 C-terminus have an additional role within the spindle assembly checkpoint, apart from recruiting Mad1 and Mad2 to kinetochores.

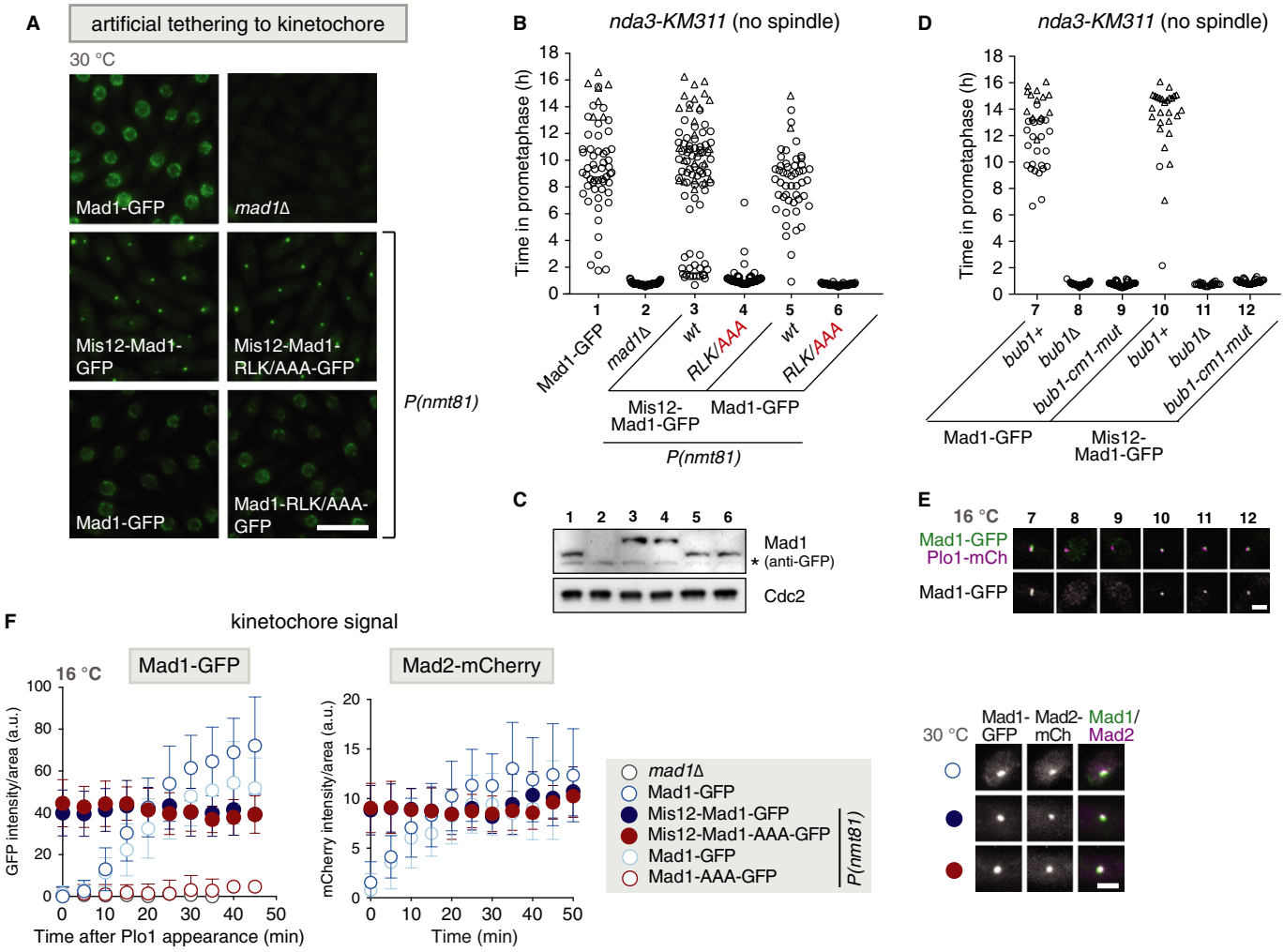

Figure 2. The Mad1 RLK motif and Bub1-cm1 have a role in signalling beyond their role in Mad1 kinetochore localization.

A Representative images of cells expressing *nda3-KM311* and the indicated GFP fusion proteins. Cells were imaged at the permissive temperature for *nda3-KM311* (30°C). Fusion to the kinetochore protein Mis12 artificially tethers Mad1 to the kinetochore. Some constructs were expressed from the inducible *nmt81* promoter, *P(nmt81)*; the endogenous *mad1* gene was deleted in these strains. Scale bar: 10 μm.

B Checkpoint function of cells expressing *plo1+-mCherry*, *nda3-KM311* and the indicated Mad1-GFP fusion proteins [same strains as in (A)] was analysed at 16°C as in Fig 1F.

C Immunoblotting of cell extracts using anti-GFP and anti-Cdc2 (loading control) antibodies. Strains are the same as in (A) and (B). The asterisk indicates a cross-reaction of the antibody.

D Checkpoint function of cells expressing *plo1+-mCherry*, *nda3-KM311* and the indicated *bub1* variants and Mad1-GFP fusion proteins was analysed as in Fig 1F.

E Representative nuclei of mitotic cells of the strains analysed in (D). Scale bar: 2 μm.

F Mad1-GFP (from cells in (B)) or Mad2-mCherry signals were quantified at the kinetochore as cells entered mitosis (a.u. = arbitrary units; error bars = s.d.; $n \geq 20$ cells). Representative nuclei are shown on the right. (Scale bar: 2 μm; see Supplementary Fig S3C for a larger field of view).

Source data are available online for this figure.

Mutations in the C-terminus of Mad1 abolish checkpoint signalling although kinetochore localization of Bub1, Mad1 and Mad2 is intact

If Bub1 and Mad1 have an additional role in the checkpoint, unrelated to Mad1 kinetochore localization, it should be possible to identify separation-of-function mutants that preserve kinetochore localization but are deficient in checkpoint signalling. We screened for such mutations in the structured and conserved C-terminus of Mad1. An initial screen narrowed down the region of interest to the very C-terminus (Supplementary Fig S4A). We noticed a conserved, negatively charged surface patch on "top" of the Mad1 "head," which we either mutated (EDD/QNN) or which we removed by truncating the protein before the last α helix (Δhelix) (Fig 3A). Both mutants maintained Mad1 kinetochore localization (Fig 3B and C), but strongly or entirely lost checkpoint activity (Fig 3D), despite being present at similar levels as wild-type Mad1 (Fig 3E). Both immunoprecipitation (Fig 3F) and co-recruitment to the kinetochore (Fig 3G, Supplementary Fig S4C) demonstrated that the interaction of Mad1 with Mad2 was largely preserved. In addition, Bub1 still

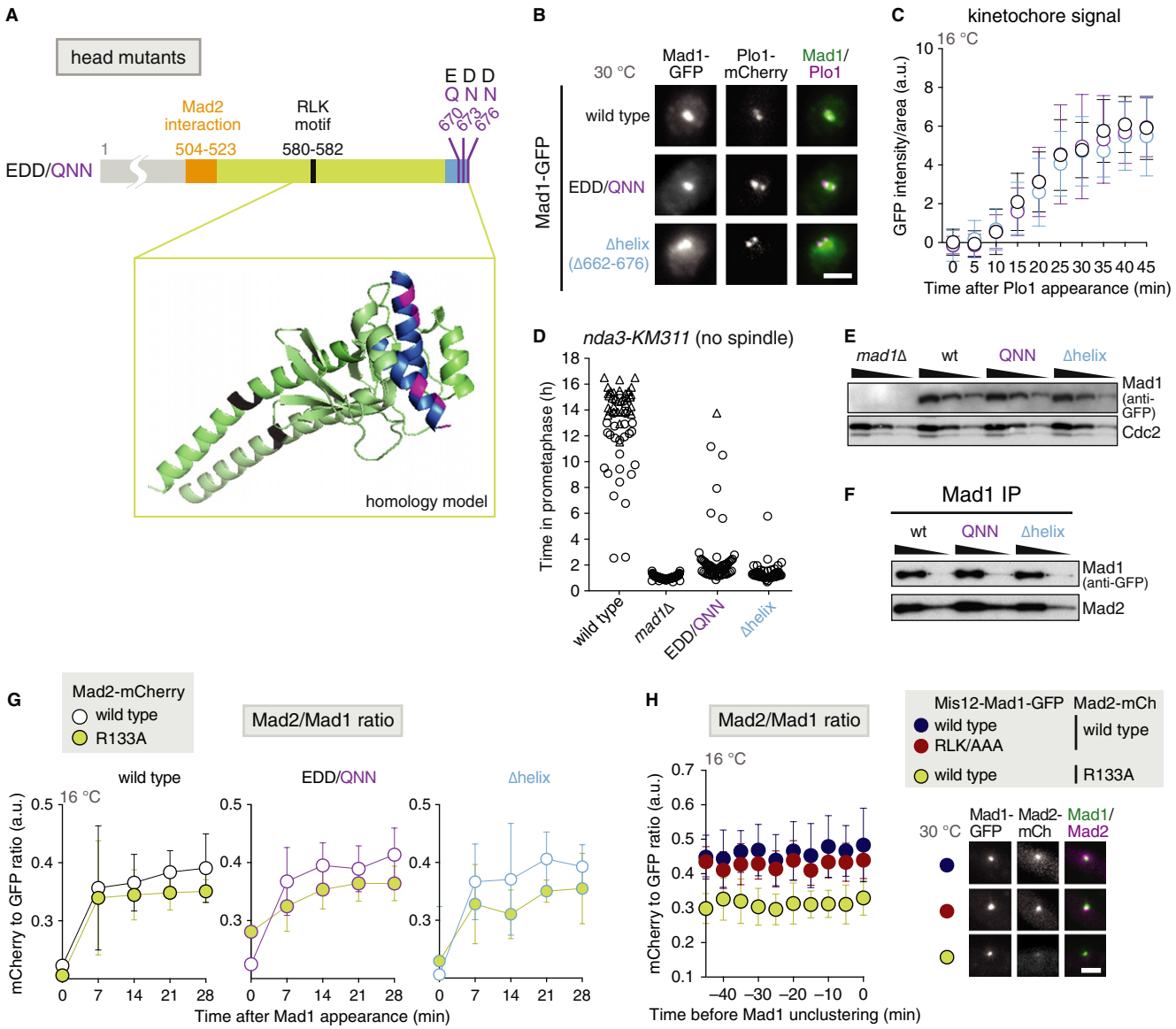

Figure 3. The top of the globular C-terminal head of Mad1 is required for checkpoint signalling, but not for kinetochore localization of Mad1:Mad2.

A Position of the head mutations in Mad1. The inset shows a homology model of the C-terminus of *Schizosaccharomyces pombe* Mad1 (aa 562-676) based on the crystal structure of the dimeric *H. sapiens* Mad1 C-terminal domain (PDB code: 4ZDO, [12]). (black: RLK motif (aa 580-582); blue: last helix of the C-terminal head (aa 662-676); purple: aa E670/D673/D676).

B Cells expressing *plo1+-mCherry*, *nda3-KM311* and the indicated Mad1-GFP fusion proteins were imaged as in Fig 1C. Representative nuclei of mitotic cells are shown (scale bar: 2 μm; see Supplementary Fig S4B for a larger field of view).

C The same strains as in (B) were analysed at the restrictive temperature for *nda3-KM311* (16°C) as in Fig 1D. Mad1-GFP signals were quantified at the kinetochore as cells entered mitosis (a.u. = arbitrary units; error bars = s.d.; $n \geq 22$ cells).

D Checkpoint function of the indicated strains was analysed at 16°C as in Fig 1F.

E Immunoblotting of cell extracts using anti-GFP and anti-Cdc2 (loading control) antibodies. A dilution series was loaded for each strain to compare intensities. Strains are the same as in (D).

F Anti-Mad1 immunoprecipitations of the indicated strains were analysed for the presence of Mad1 and Mad2 using anti-GFP and anti-Mad2 antibodies. Input and flow through of the immunoprecipitation are shown in Supplementary Fig S4D.

G Cells expressing *nda3-KM311*, the indicated *mad1-GFP* constructs and either *mad2+-mCherry* or *mad2-R133A-mCherry* were followed by live-cell imaging at 16°C. The Mad2-mCherry/Mad1-GFP ratio at kinetochores was determined as cells entered mitosis (a.u. = arbitrary units; error bars = s.d.). Mad1-wt + Mad2-wt: $n = 13$; Mad1-wt + Mad2-R133A: $n = 21$; Mad1-QNN + Mad2-wt: $n = 16$; Mad1-QNN + Mad2-R133A: $n = 14$; Mad1-Δhelix + Mad2-wt: $n = 10$; Mad1-Δhelix + Mad2-R133A: $n = 8$; statistical analysis in Supplementary Fig S4E. Representative images for Mad1-GFP and Mad2-mCherry localization in Supplementary Fig S4C.

H Strains were followed by live-cell imaging as in (G) and Fig 2F. The Mad2-mCherry/Mad1-GFP ratio at kinetochores was determined as cells entered mitosis (a.u. = arbitrary units; error bars = s.d.; $n \geq 14$ cells; statistical analysis in Supplementary Fig S4F). Representative nuclei are shown on the right (scale bar: 2 μm).

Source data are available online for this figure.

localized to kinetochores (Supplementary Fig S4G). Hence, in these Mad1 mutants Bub1, Mad1 and Mad2 are at kinetochores; yet, checkpoint signalling is strongly impaired.

The C-terminal part of Mad1 (α3 and head) has been proposed to fold back onto Mad1-α2 [2], which would bring the Mad1 head in close vicinity to Mad2. Because Mad1-bound Mad2 needs to dimerize with additional Mad2 to support checkpoint function [3,21], we suspected that the Mad1 C-terminal head promotes this dimerization. As in human cells [22], the Mad2/Mad1 ratio at kinetochores is reduced in a dimerization-deficient Mad2 mutant (Mad2-R133A [23]; Fig 3G), presumably because Mad2 cannot be recruited to the kinetochore through Mad2:Mad2 dimerization, but only through binding to Mad1. In both the Mad1-EDD/QNN and -Δhelix mutant, the Mad2/Mad1 ratio at kinetochores was similar to Mad1 wild-type cells, and in both mutants, there was less Mad2 relative to Mad1 at kinetochores when the Mad2-R133A mutant was expressed instead of wild-type Mad2 (Fig 3G). This strongly indicates that Mad2 dimerization is intact. Similarly, the Mad2/Mad1 ratio after artificially tethering Mad1-RLK/AAA was more similar to wild-type than to Mad2-R133A-expressing cells (Fig 3H). Hence, the Mad1 C-terminal head and the RLK motif promote checkpoint function, but seemingly not through facilitating Mad2 dimerization.

Our data indicate that the C-terminal head of Mad1 has a previously unrecognized role in checkpoint signalling, which is neither related to the requirement for the C-terminus to bring Mad1 to kinetochores (Fig 1) nor related to the role of Mad1 in recruiting Mad2, either directly or through Mad2:Mad2 dimerization (Figs 2 and 3). Since very similar findings have been made in human cells [11], this function of Mad1 is probably conserved across eukaryotes. Current models for the spindle assembly checkpoint mainly see Mad1 as a passive platform for presenting Mad2 at kinetochores. Our findings revise this picture and make Mad1 an active player in checkpoint signalling. How the Mad1 C-terminus promotes checkpoint activity and how Bub1 fits into the picture remains unclear (Fig 4). Our finding that the very C-terminal Mad1 head is required for checkpoint activity without being required for any of the known Mad1 functions provides a basis to elucidate the molecular mechanism. How the head is arranged with respect to the remainder of the molecule is still unclear (Fig 4). In any case, we suspect that the head, like similar folds in other kinetochore proteins [24–27], mediates a protein–protein interaction (Fig 4B). The interacting partner could be Mad2 or another (checkpoint) protein. Although we find Mad2 dimerization apparently intact in the Mad1-EDD/QNN, Mad1-Δhelix or Mad1-RLK/AAA mutant (Fig 3), it remains possible that these regions are involved in promoting the conformational change of Mad2 that is required for binding of free Mad2 to Cdc20 [28,29] (Fig 4B). It would be interesting to perform cross-linking experiments to determine which arrangement the Mad1 C-terminus takes *in vivo* and which proteins the different regions interact with (Fig 4B).

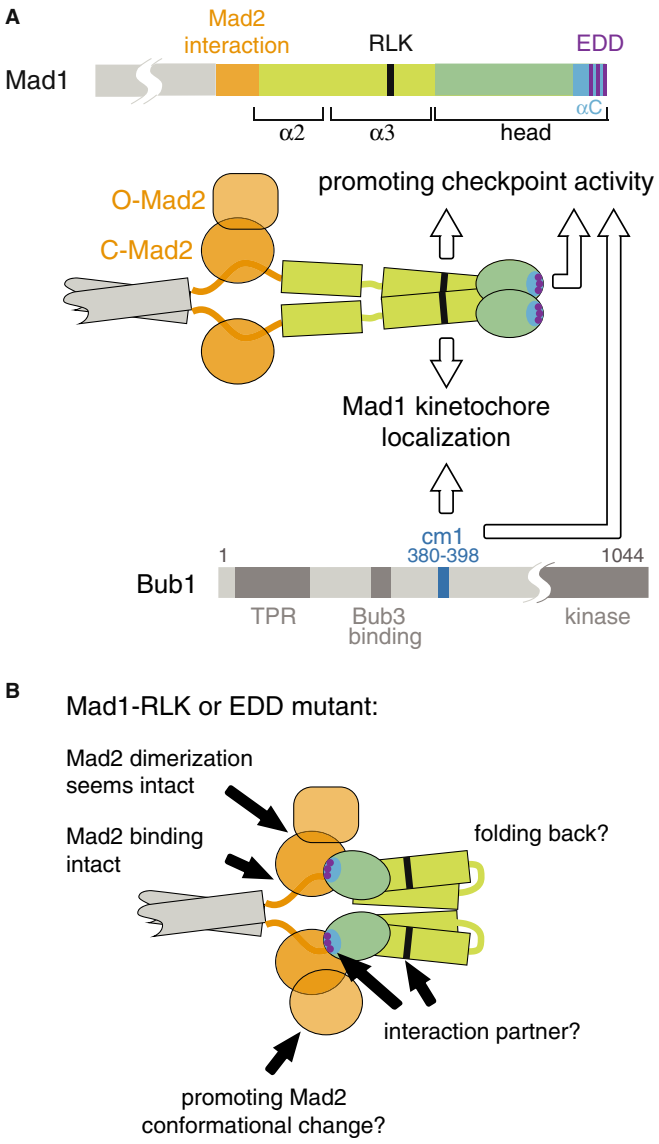

Figure 4. Mad1 C-terminus and Bub1-cm1 promote checkpoint signalling independently of their role in Mad1:Mad2 kinetochore recruitment.

A Schematic of the Mad1 and Bub1 proteins with suggested functions for the Mad1-RLK motif, the Mad1 C-terminal head and Bub1-cm1.

B It is unknown how Mad1 α3 and head arrange with respect to α2. A straight conformation is shown in (A), folding back [2] is shown in (B). How the Mad1 C-terminus promotes checkpoint signalling remains unclear. Findings and ideas are indicated by black arrows and discussed in the text.

Materials and Methods

Schizosaccharomyces pombe strains

Strains are listed in Supplementary Table 1. For the amino acid (aa) numbering of Mad1, note that we corrected the annotation of the start codon, which shifted by 13 aa (Supplementary Information).

In general, mutants were integrated into the endogenous locus using PCR-based gene targeting [30] and replaced the wild-type allele. *P(nmt81)-(mis12-)mad1-(AAA)-GFP* constructs were integrated into the *leu1* locus using the pDUAL system [31], and the endogenous *mad1+* gene was deleted. *Schizosaccharomyces pombe* strains with the following mutations or modifications have been described: *nda3-KM311* [32], *mad1+-GFP≪kanR*, *mad2+-GFP≪kanR*, *mad3+-GFP≪kanR*, *plo1+-mCherry*, *ark1+*-GFP [7], *bub1+-GFP≪kanR* [33], *bub3+-GFP≪kanR* [10], *mad1Δ::ura4+* [34], *bub1Δ::ura4+* [35].

Culture conditions

For live-cell imaging, cells were grown at 30°C in either rich medium (YEA) or Edinburgh minimal medium (EMM) containing the necessary supplements. Mad1 constructs expressed from *P(nmt81)* at the *leu1* locus were cultured for 19 h in EMM without thiamine to induce expression, then washed three times with EMM containing 16 μM thiamine and resuspended in EMM containing 16 μM thiamine before shifting to 16°C for imaging.

Live-cell imaging to assess checkpoint functionality

Live-cell imaging was performed on a DeltaVision microscope (Applied Precision/GE Healthcare) as previously described [7].

Quantification of GFP and mCherry signals in the nucleus and at the kinetochore

To determine the intensity of checkpoint protein-GFP or -mCherry signals at the kinetochores, mitotic cells were identified by the appearance of localized Plo1-mCherry signal at SPBs, or by localized Mad1-GFP or Mad2-mCherry signal at kinetochores. In cells expressing constitutive kinetochore-tethered Mad1 (Mis12-Mad1) and lacking a fluorescent tag on Plo1 (so that entry into mitosis could not be judged), signals were measured for 50 min before the kinetochores unclustered. The unclustering (Supplementary Fig S2D) indicates that the cell is in mitosis. An area was placed around kinetochores (for checkpoint protein-GFP or -mCherry strains) or SPBs (for Plo1-mCherry strains; because kinetochores cluster at the SPB in early mitosis, this captures the signal at kinetochores). The GFP or mCherry signal in this area was traced over time. To determine signal intensity at the kinetochore, the total signal intensity per area of a similarly sized region in the nucleoplasm was subtracted from the total signal intensity per area around the kinetochore.

Fluorescence microscopy of asynchronous cell cultures

Images of living cells were acquired with a CoolSnap EZ (Roper) camera using a 63 × /1.4 Plan Apochromat oil objective on a Zeiss AxioImager microscope and were processed with MetaMorph software (Molecular Devices Corporation). Typically, a Z-stack of about 3 μm thickness, with single planes spaced by 0.3 μm, was acquired and subsequently projected. Shown are sum intensity projections of the Z-stack for checkpoint proteins and maximum intensity projections of the Z-stack for Plo1.

Immunoprecipitation

Immunoprecipitation was performed as previously described [10] using rabbit anti-Mad1 [10] or mouse anti-GFP (Roche, 11814460001) antibodies and protein A-coated magnetic beads (Dynabeads, Invitrogen 10002D).

Cell extracts, SDS–PAGE and immunoblotting

Protein extraction was performed as previously described [7]. Mouse anti-GFP (Roche, 11814460001), rabbit anti-Mad1 [10], rabbit anti-Mad2 [36], mouse anti-HA (Roche, 12CA5) or rabbit anti-Cdc2 (Santa Cruz, SC-53) were used as primary antibodies. Secondary antibodies were anti-mouse or anti-rabbit HRP conjugates (Dianova, 115-035-003, 111-035-003) and were read out using chemiluminescence.

Supplementary information for this article is available online: http://embor.embopress.org

Acknowledgements

We thank Jan Hasenauer for statistical analysis, Julia Kamenz for valuable suggestions, Katrin Bertram, Holda Anagho, Eva Illgen, Julia Binder, Julia Sauerwald, Alexandra Dudek and Philipp Spät for excellent technical help, Andrei Lupas for advice on coiled-coil truncations, the Proteome Center of the University of Tübingen for mass spectrometric analysis and Jakob Nilsson and his group for communicating unpublished results. We are grateful for funding by the Max Planck Society; St.H. was additionally supported by the Ernst Schering Foundation.

Author contributions

SHe (Figs 1–3, Supplementary Figs S1–4), KS (Figs 1–3, Supplementary Figs S1–4), HW (Fig 1), ML (Figs 1 and 2, Supplementary Fig S4), NS (Fig 1, Supplementary Figs S1 and 3) and NH (Supplementary Fig S3) designed and performed experiments; SHa devised the project and wrote the manuscript together with SHe and input from all other authors.

Conflict of interest

The authors declare that they have no conflict of interest.

References

1. Lara-Gonzalez P, Westhorpe FG, Taylor SS (2012) The spindle assembly checkpoint. *Curr Biol* 22: R966 – R980
2. Sironi L, Mapelli M, Knapp S, De Antoni A, Jeang KT, Musacchio A (2002) Crystal structure of the tetrameric Mad1-Mad2 core complex: implications of a safety belt binding mechanism for the spindle checkpoint. *EMBO J* 21: 2496 – 2506
3. De Antoni A, Pearson CG, Cimini D, Canman JC, Sala V, Nezi L, Mapelli M, Sironi L, Faretta M, Salmon ED, Musacchio A (2005) The Mad1/Mad2 complex as a template for Mad2 activation in the spindle assembly checkpoint. *Curr Biol* 15: 214 – 225
4. Primorac I, Musacchio A (2013) Panta rhei: the APC/C at steady state. *J Cell Biol* 201: 177 – 189
5. Chao WC, Kulkarni K, Zhang Z, Kong EH, Barford D (2012) Structure of the mitotic checkpoint complex. *Nature* 484: 208 – 213
6. Jia L, Kim S, Yu H (2013) Tracking spindle checkpoint signals from kinetochores to APC/C. *Trends Biochem Sci* 38: 302 – 311
7. Heinrich S, Windecker H, Hustedt N, Hauf S (2012) Mph1 kinetochore localization is crucial and upstream in the hierarchy of spindle assembly checkpoint protein recruitment to kinetochores. *J Cell Sci* 125: 4720 – 4727
8. Emre D, Terracol R, Poncet A, Rahmani Z, Karess RE (2011) A mitotic role for Mad1 beyond the spindle checkpoint. *J Cell Sci* 124: 1664 – 1671
9. Mariani L, Chiroli E, Nezi L, Muller H, Piatti S, Musacchio A, Ciliberto A (2012) Role of the Mad2 dimerization interface in the spindle assembly checkpoint independent of kinetochores. *Curr Biol* 22: 1900 – 1908

10. Heinrich S, Geissen EM, Kamenz J, Trautmann S, Widmer C, Drewe P, Knop M, Radde N, Hasenauer J, Hauf S (2013) Determinants of robustness in spindle assembly checkpoint signalling. *Nat Cell Biol* 15: 1328 – 1339
11. Kruse T, Larsen MSY, Sedgwick GG, Sigurdsson JO, Streicher W, Olsen JV, Nilsson J (2014) A direct role of Mad1 in the spindle assembly checkpoint beyond Mad2 kinetochore recruitment. *EMBO Rep* DOI 10.1002/embr.201338101
12. Kim S, Sun H, Tomchick DR, Yu H, Luo X (2012) Structure of human Mad1 C-terminal domain reveals its involvement in kinetochore targeting. *Proc Natl Acad Sci USA* 109: 6549 – 6554
13. Kastenmayer JP, Lee MS, Hong AL, Spencer FA, Basrai MA (2005) The C-terminal half of *Saccharomyces cerevisiae* Mad1p mediates spindle checkpoint function, chromosome transmission fidelity and CEN association. *Genetics* 170: 509 – 517
14. Scott RJ, Lusk CP, Dilworth DJ, Aitchison JD, Wozniak RW (2005) Interactions between Mad1p and the nuclear transport machinery in the yeast *Saccharomyces cerevisiae*. *Mol Biol Cell* 16: 4362 – 4374
15. Chung E, Chen RH (2002) Spindle checkpoint requires Mad1-bound and Mad1-free Mad2. *Mol Biol Cell* 13: 1501 – 1511
16. Martin-Lluesma S, Stucke VM, Nigg EA (2002) Role of Hec1 in spindle checkpoint signaling and kinetochore recruitment of Mad1/Mad2. *Science* 297: 2267 – 2270
17. Brady DM, Hardwick KG (2000) Complex formation between Mad1p, Bub1p and Bub3p is crucial for spindle checkpoint function. *Curr Biol* 10: 675 – 678
18. Warren CD, Brady DM, Johnston RC, Hanna JS, Hardwick KG, Spencer FA (2002) Distinct chromosome segregation roles for spindle checkpoint proteins. *Mol Biol Cell* 13: 3029 – 3041
19. Chen RH, Brady DM, Smith D, Murray AW, Hardwick KG (1999) The spindle checkpoint of budding yeast depends on a tight complex between the Mad1 and Mad2 proteins. *Mol Biol Cell* 10: 2607 – 2618
20. Klebig C, Korinth D, Meraldi P (2009) Bub1 regulates chromosome segregation in a kinetochore-independent manner. *J Cell Biol* 185: 841 – 858
21. Nezi L, Rancati G, De Antoni A, Pasqualato S, Piatti S, Musacchio A (2006) Accumulation of Mad2-Cdc20 complex during spindle checkpoint activation requires binding of open and closed conformers of Mad2 in *Saccharomyces cerevisiae*. *J Cell Biol* 174: 39 – 51
22. Hewitt L, Tighe A, Santaguida S, White AM, Jones CD, Musacchio A, Green S, Taylor SS (2010) Sustained Mps1 activity is required in mitosis to recruit O-Mad2 to the Mad1-C-Mad2 core complex. *J Cell Biol* 190: 25 – 34
23. Sironi L, Melixetian M, Faretta M, Prosperini E, Helin K, Musacchio A (2001) Mad2 binding to Mad1 and Cdc20, rather than oligomerization, is required for the spindle checkpoint. *EMBO J* 20: 6371 – 6382
24. Wei RR, Schnell JR, Larsen NA, Sorger PK, Chou JJ, Harrison SC (2006) Structure of a central component of the yeast kinetochore: the Spc24p/Spc25p globular domain. *Structure* 14: 1003 – 1009
25. Ciferri C, Pasqualato S, Screpanti E, Varetti G, Santaguida S, Dos Reis G, Maiolica A, Polka J, De Luca JG, De Wulf P, Salek M, Rappsilber J, Moores CA, Salmon ED, Musacchio A (2008) Implications for kinetochore-microtubule attachment from the structure of an engineered Ndc80 complex. *Cell* 133: 427 – 439
26. Corbett KD, Yip CK, Ee LS, Walz T, Amon A, Harrison SC (2010) The monopolin complex crosslinks kinetochore components to regulate chromosome-microtubule attachments. *Cell* 142: 556 – 567
27. Schmitzberger F, Harrison SC (2012) RWD domain: a recurring module in kinetochore architecture shown by a Ctf19-Mcm21 complex structure. *EMBO Rep* 13: 216 – 222
28. Luo X, Yu H (2008) Protein metamorphosis: the two-state behavior of Mad2. *Structure* 16: 1616 – 1625
29. Mapelli M, Musacchio A (2007) MAD contortions: conformational dimerization boosts spindle checkpoint signaling. *Curr Opin Struct Biol* 17: 716 – 725
30. Bahler J, Wu JQ, Longtine MS, Shah NG, McKenzie A III, Steever AB, Wach A, Philippsen P, Pringle JR (1998) Heterologous modules for efficient and versatile PCR-based gene targeting in *Schizosaccharomyces pombe*. *Yeast* 14: 943 – 951
31. Matsuyama A, Shirai A, Yashiroda Y, Kamata A, Horinouchi S, Yoshida M (2004) pDUAL, a multipurpose, multicopy vector capable of chromosomal integration in fission yeast. *Yeast* 21: 1289 – 1305
32. Hiraoka Y, Toda T, Yanagida M (1984) The NDA3 gene of fission yeast encodes beta-tubulin: a cold-sensitive nda3 mutation reversibly blocks spindle formation and chromosome movement in mitosis. *Cell* 39: 349 – 358
33. Yamaguchi S, Decottignies A, Nurse P (2003) Function of Cdc2p-dependent Bub1p phosphorylation and Bub1p kinase activity in the mitotic and meiotic spindle checkpoint. *EMBO J* 22: 1075 – 1087
34. Vanoosthuyse V, Valsdottir R, Javerzat JP, Hardwick KG (2004) Kinetochore targeting of fission yeast Mad and Bub proteins is essential for spindle checkpoint function but not for all chromosome segregation roles of Bub1p. *Mol Cell Biol* 24: 9786 – 9801
35. Bernard P, Hardwick K, Javerzat JP (1998) Fission yeast bub1 is a mitotic centromere protein essential for the spindle checkpoint and the preservation of correct ploidy through mitosis. *J Cell Biol* 143: 1775 – 1787
36. Yamada HY, Matsumoto S, Matsumoto T (2000) High dosage expression of a zinc finger protein, Grt1, suppresses a mutant of fission yeast slp1(+), a homolog of CDC20/p55CDC/Fizzy. *J Cell Sci* 113(Pt 22): 3989 – 3999
37. Mulvihill DP, Petersen J, Ohkura H, Glover DM, Hagan IM (1999) Plo1 kinase recruitment to the spindle pole body and its role in cell division in *Schizosaccharomyces pombe*. *Mol Biol Cell* 10: 2771 – 2785

